

AD-A141 537

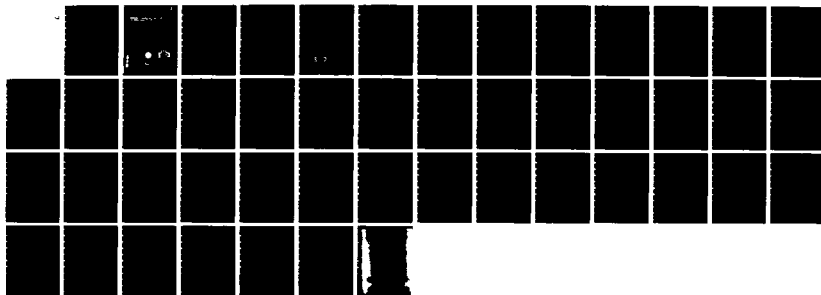
MECHANISM OF OPERATION AND DESIGN CONSIDERATIONS FOR  
SURFACE ACOUSTIC WAV. (U) NAVAL RESEARCH LAB WASHINGTON  
DC H WOHLTJEN 23 APR 84 NRL-AR-5314 SBI-AD-E000 568

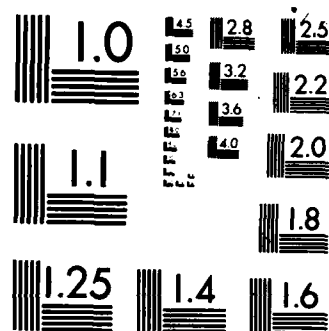
1/1

UNCLASSIFIED

F/G 14/2

NL





2

NRL Memorandum Report 5314

# Operation and Design Considerations of Acoustic Wave Device Vapor Sensors

R. WOHLTEN

Hughes Aircraft Company  
Aircraft Division

AD-A141 537

June 21, 1964

DTIC  
ELECTE  
NO 24 004

B

NAVY RESEARCH LABORATORY  
Washington, D.C.

Reproduction of this report is unlimited.

84 05 24 064

AD-A141 537

SECURITY CLASSIFICATION OF THIS PAGE

| REPORT DOCUMENTATION PAGE  |  |   |   |                                    |
|--|--|---|---|------------------------------------|
| 1a. REPORT SECURITY CLASSIFICATION<br><b>UNCLASSIFIED</b>  |  | 1b. RESTRICTIVE MARKINGS  |   |                                    |
| 2a. SECURITY CLASSIFICATION AUTHORITY  |  | 3. DISTRIBUTION AVAILABILITY OF REPORT  |   |                                    |
| 2b. DECLASSIFICATION/DOWNGRADING SCHEDULE  |  | Approved for public release; distribution unlimited.                              |   |                                    |
| 4. PERFORMING ORGANIZATION REPORT NUMBER(S)<br><b>NRL Memorandum Report 5314</b>   |  | 5. MONITORING ORGANIZATION REPORT NUMBER(S)                                       |   |                                    |
| 6a. NAME OF PERFORMING ORGANIZATION<br><b>Naval Research Laboratory</b>  | 6b. OFFICE SYMBOL<br>(If applicable)<br><b>Code 6170</b> | 7a. NAME OF MONITORING ORGANIZATION   |   |                                    |
| 6c. ADDRESS (City, State and ZIP Code)<br><b>Washington, DC 20375</b>  |  | 7b. ADDRESS (City, State and ZIP Code)  |   |                                    |
| 8a. NAME OF FUNDING/SPONSORING ORGANIZATION<br><b>U.S. Army Chemical R&amp;D Center</b>  | 8b. OFFICE SYMBOL<br>(If applicable)                     | 9. PROCUREMENT INSTRUMENT IDENTIFICATION NUMBER<br><b>ARMY CRDC 61102A</b>        |   |                                    |
| 8c. ADDRESS (City, State and ZIP Code)<br><b>Aberdeen Proving Ground, MD 21010</b>   |  | 10. SOURCE OF FUNDING NOS.  |   |                                    |
| 11. TITLE (Include Security Classification)<br><b>(See page ii)</b>  |  | PROGRAM ELEMENT NO.<br><b>61102A</b>  | PROJECT NO.   | TASK NO.                           |
|  |  |   |   | WORK UNIT NO.<br><b>61-1439-04</b> |
| 12. PERSONAL AUTHOR(S)<br><b>H. Wohltjen</b>   |  |   |   |                                    |
| 13a. TYPE OF REPORT<br><b>Progress report</b>  | 13b. TIME COVERED<br><b>FROM 10/82 TO 10/83</b>          | 14. DATE OF REPORT (Yr., Mo., Day)<br><b>April 23, 1984</b>                       |   | 15. PAGE COUNT<br><b>45</b>        |
| 16. SUPPLEMENTARY NOTATION   |  |   |   |                                    |
| 17. COSATI CODES   |  | 18. SUBJECT TERMS (Continue on reverse if necessary and identify by block number) |   |                                    |
| FIELD  | GROUP  | SUB-GR  |   |                                    |
|  |  |   | Surface acoustic wave device    Vapor detection    SAW oscillator |                                    |
|  |  |   | Chemical microsensor    Thin films                                |                                    |
| 19. ABSTRACT (Continue on reverse if necessary and identify by block number)   |  |   |   |                                    |
| <p>Surface acoustic wave (SAW) devices offer many attractive features for application as vapor phase chemical microsensors. This paper describes the characteristics of SAW devices and techniques by which they can be employed as vapor sensors. The perturbation of SAW amplitude and velocity by polymeric coating films was investigated both theoretically and experimentally. Highest sensitivity can be achieved when the device is used as the resonating element in a delay line oscillator circuit. A simple equation has been developed from theoretical considerations which offers reasonably accurate quantitative predictions of SAW device frequency shifts when subjected to a given mass loading. In this mode the SAW device behaves in a fashion very similar to conventional bulk wave quartz crystal microbalances except that the sensitivity can be several orders of magnitude higher and the device size can be several orders of magnitude smaller. Detection of mass changes of less than 1 femtogram by a SAW device having a surface area of <math>10^{-4}</math> cm<sup>2</sup> is theoretically possible.</p> |  |   |   |                                    |
| 20. DISTRIBUTION AVAILABILITY OF ABSTRACT<br>UNCLASSIFIED UNLIMITED <input checked="" type="checkbox"/> SAME AS RPT <input type="checkbox"/> DTIC USERS <input type="checkbox"/>   |  | 21. ABSTRACT SECURITY CLASSIFICATION<br><b>UNCLASSIFIED</b>                       |   |                                    |
| 22a. NAME OF RESPONSIBLE INDIVIDUAL<br><b>H. Wohltjen</b>  |  | 22b. TELEPHONE NUMBER<br>(Include Area Code)<br><b>(202) 767-2536</b>             | 22c. OFFICE SYMBOL<br><b>Code 6170</b>                            |                                    |

DD FORM 1473, 83 APR

EDITION OF 1 JAN 73 IS OBSOLETE

SECURITY CLASSIFICATION OF THIS PAGE

SECURITY CLASSIFICATION OF THIS PAGE

**11. TITLE (Include Security Classification)**

**MECHANISM OF OPERATION AND DESIGN CONSIDERATIONS FOR SURFACE ACOUSTIC WAVE  
DEVICE VAPOR SENSORS**

SECURITY CLASSIFICATION OF THIS PAGE

## CONTENTS

|  |    |
|--|----|
| INTRODUCTION .....                           | 1  |
| RAYLEIGH SURFACE WAVE CHARACTERISTICS .....  | 3  |
| THEORY OF SAW INTERACTIONS .....             | 10 |
| SAW Amplitude Perturbations .....            | 10 |
| SAW Velocity (Frequency) Perturbations ..... | 14 |
| EXPERIMENTAL SECTION .....                   | 19 |
| RESULTS AND DISCUSSION .....                 | 20 |
| SAW Amplitude Measurements .....             | 20 |
| SAW Frequency Measurements .....             | 25 |
| SAW Vapor Sensor Considerations .....        | 32 |
| Ultimate Performance Limits .....            | 35 |
| CONCLUSION .....                             | 39 |
| ACKNOWLEDGMENT .....                         | 40 |
| LITERATURE CITED .....                       | 41 |

**DTIC**  
**ELECTE**  
**S** MAY 24 1984 **D**  
**B**



|                    |                                     |
|--------------------|-------------------------------------|
| Accession For      |                                     |
| NTIS GRA&I         | <input checked="" type="checkbox"/> |
| DTIC TAB           | <input type="checkbox"/>            |
| Unannounced        | <input type="checkbox"/>            |
| Justification      |                                     |
| By _____           |                                     |
| Distribution/      |                                     |
| Availability Codes |                                     |
| Dist               | Avail and/or Special                |
| A-1                |                                     |

Mechanism of Operation and Design Considerations  
for Surface Acoustic Wave Device Vapor Sensors

Hank Wohltjen

Naval Research Laboratory  
Chemistry Division  
Code 6170  
Washington, D. C. 20375

INTRODUCTION

The phenomenon of waves which occur on the surface of solids was first described by Lord Rayleigh in 1885(1). Subsequent studies of surface waves were conducted primarily by seismologists who were interested in the propagation of mechanical waves at the earth's surface (i.e. earthquakes). In 1965 White and Voltmer(2) developed the interdigital transducer which allows the convenient generation of surface waves in piezoelectric solids. This breakthrough precipitated a considerable amount of work in the application of surface acoustic wave (SAW) methods to radio frequency signal processing. Here the small size, high performance and relative simplicity of SAW filters, delay lines and convolvers found many applications particularly in electronic countermeasure systems for aerospace use(3,4).

The first report of a sensor for chemical vapors based on SAW device technology appeared in 1979(5,6). Both quartz and  $\text{LiNbO}_3$  SAW devices were evaluated for their performance as detectors in a gas chromatograph system when coated with sensitizing organic films. Investigations of SAW vapor sensing using polyvinyl chloride films have been reported by Fertsch, White

Manuscript approved January 27, 1984.

and Muller(7,8). A comparison of bulk wave and surface wave device sensors for  $\text{SO}_2$  was made by Bryant, Lee and Vetelino(9). The surface wave device was found to detect less than 100 ppb of  $\text{SO}_2$  which was at least an order of magnitude more sensitive than the bulk wave sensor. Recently a clever scheme for SAW vapor sensing using a thin membrane device has been reported by Chuang, White and Bernstein(10) and a hydrogen sensor using a palladium coated SAW device has been described by D'Amico, Palma and Verona(12).

SAW devices as chemical sensors are attractive because of their small size (e.g.  $<0.1\text{cm}^3$ ), ruggedness, low cost, electronic output, sensitivity and adaptability to a wide variety of vapor phase analytical problems.



## RAYLEIGH SURFACE WAVE CHARACTERISTICS

The displacement of particles near the surface of a solid which is propagating a Rayleigh surface wave is shown in figure 1. The particle displacements have two components; a longitudinal component (i.e. back and forth, parallel to the surface) and a shear vertical component (i.e. up and down). The superposition of these two components results in surface particle trajectories which follow a retrograde elliptical path around their quiescent positions. As suggested by their name, these surface waves have most of their energy localized within one or two acoustic wavelengths of the surface. This permits easy and strong interaction with the medium adjacent to the surface. (Surface acoustic waves can also have an associated electric field if they are generated on a piezoelectric substrate.) Other particle displacements are possible (e.g. shear horizontal rather than shear vertical) but such waves are not Rayleigh waves. Consideration of these other wave types (e.g. Love waves, Stonely waves, etc.) is beyond the scope of this discussion.

The primary reason for focusing on Rayleigh waves is that they are generated quite readily in a variety of piezoelectric substrates using an interdigital transducer electrode (IDT). The interdigital electrode is fabricated from a thin film of metal (typically 1000-2000 Å thick) which is vacuum evaporated onto the polished piezoelectric substrate. The metal film is covered with a photoresist film and then exposed with light through a mask having the desired IDT pattern. The resist is developed, exposing areas of the metal which can then be etched away in an appropriate etchant to produce the IDT electrodes. For very small IDT structures electron beam lithography and plasma etching are frequently employed. Once fabricated, these electrodes will generate a Rayleigh surface wave in the piezoelectric substrate if a radio frequency (RF) voltage is applied. The time varying

## SURFACE PARTICLE DISPLACEMENT

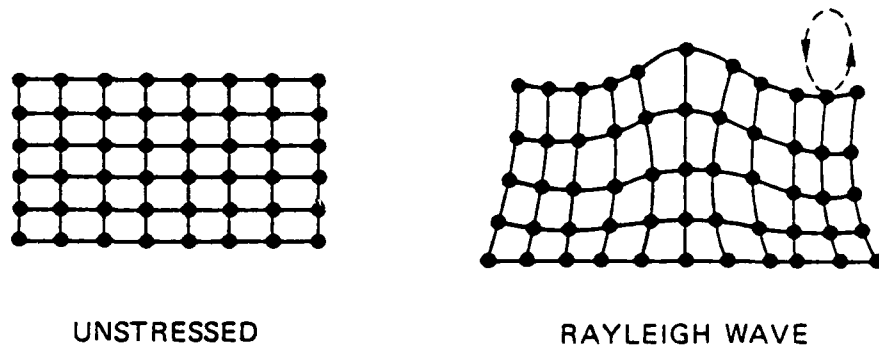


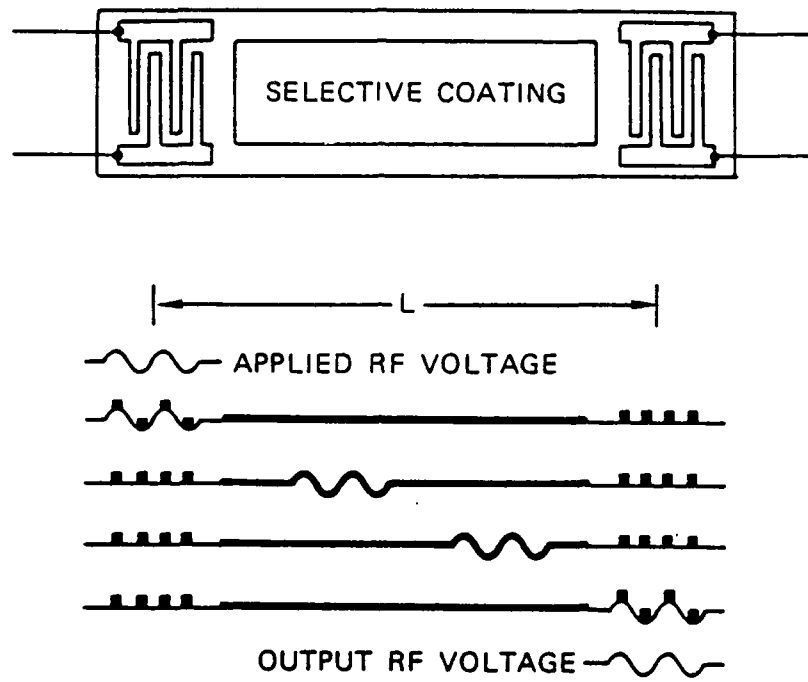
Figure 1. Deformation of the SAW substrate resulting from the propagation of a Rayleigh surface wave. The vertical displacement amplitude is typically about  $10\text{\AA}$ .

voltage will result in a synchronously varying deformation of the piezoelectric substrate and the subsequent generation of a propagating Rayleigh surface wave. The wavelength (and hence the operating frequency) of the Rayleigh wave is determined by the spacing between the electrodes. The electrical impedance of the IDT on a given substrate is determined by the number of electrodes and the electrode overlap length. This overlap length also determines the width of the acoustic beam which is produced. For a typical piezoelectric substrate such as quartz which has a Rayleigh wave velocity ( $V_R$ ) of about 3100 meters/sec, an operating frequency ( $f$ ) of 31 MHz will result when the wavelength ( $\lambda$ ) of the acoustic wave is  $1 \times 10^{-4}$  meters (100 micrometers) since  $f = V_R / \lambda$ . Thus the interdigital electrode required to operate at this frequency would typically consist of a "finger" of one polarity 25 micrometers wide separated by 25 micrometers from the next finger pair. Practical microfabrication lithography limits the finger width in state-of-the-art devices to about 0.25 micrometers (i.e. 3 GHz operating frequency). A lower frequency limit for practical SAW devices is about 10 MHz. Below this frequency the devices become too large (e.g. greater than several  $\text{cm}^2$  in area). The efficiency with which the RF voltage applied to the IDT couples to the mechanical deformation depends heavily on the piezoelectric substrate material used. Quartz is not as good in this respect as other materials (such as  $\text{LiNbO}_3$ ) and as a result, requires more fingers on the IDT to achieve efficient power transfer. The operating bandwidth of an IDT is inversely related to the number of finger pairs ( $N$ ) in the electrode. A typical IDT having 50 finger pairs and operating at 30 MHz ( $f_0$ ) would have a bandwidth of about 0.6 MHz (i.e.  $f_0/N$ ) which means that the RF frequency would have to be  $30.0 \text{ MHz} \pm 0.3 \text{ MHz}$  for efficient power transfer to occur. Electrically, the IDT's appear as a

capacitive load to the RF voltage source and a series matching inductance is often employed to improve the power transfer efficiency. Further information on the design and electrical characteristics of SAW IDT's can be found in references 3, 11.

As previously mentioned, the SAW device substrate must be piezoelectric to permit the easy generation of a Rayleigh wave with an IDT electrode. Ordinarily, polished single crystal slabs of quartz or lithium niobate are used because of their desirable SAW characteristics (e.g. low cost, good piezoelectric coupling, low temperature coefficient of delay, low acoustic loss, etc.). Although other materials are available certain crystalline orientations are frequently chosen to optimize either the piezoelectric coupling coefficient or the temperature behavior of the substrate in SAW applications. For example, in quartz the Rayleigh wave velocity of the ST cut exhibits a zero temperature coefficient of delay around room temperature, whereas the YX cut has a more efficient piezoelectric coupling coefficient but a non zero temperature coefficient. Thus, the choice of substrate material depends somewhat on the intended application. The substrate surface which supports the Rayleigh wave must be very smooth to prevent energy losses from wave scattering at imperfections. Optically polished surfaces are usually adequate. Surface acoustic waves offer many attractive possibilities in the design of miniature delay lines and resonators because the wavelength of sound in the piezoelectric substrate is about  $10^5$  times smaller than that of an electromagnetic wave of the same frequency. Perhaps the simplest SAW device is a delay line (figure 2) which consists of an IDT at each end of an appropriate piezoelectric substrate. One IDT acts as a transmitter and the other and the other as a receiver of acoustic energy which travels across the substrate surface. The

# SAW DELAY LINE



$$\text{TIME DELAY } (\tau) = \frac{L}{V_R}$$

Figure 2. Top view and side view of a SAW delay line propagating a Rayleigh wave. The vertical displacement of the wave is greatly exaggerated for clarity.

propagating Rayleigh wave is free to interact with matter in contact with the delay line surface. This wave/matter interaction results in alteration of the wave's characteristics (e.g. amplitude, phase, harmonic content, etc.) and is the basis of SAW device chemical sensors.

Considering the SAW delay line in greater detail, one realizes that the delay time ( $\tau$ ) is directly related to the propagation path length (i.e. distance between IDT electrodes). A problem is encountered in the generation and detection of surface waves on delay lines which deserves attention. Namely, the simple IDT's described here are bidirectional and will permit a significant amount of energy to be reflected off the edge of the piezoelectric substrate immediately behind the electrode. This gives rise to an effect known as triple transit echo which can result in anomolous signals appearing at the receiving IDT. Triple transit echo is ordinarily eliminated by the application of acoustic energy absorbers (e.g. silicone adhesive) at the ends of the delay line. Alternatively the ends of the substrate can be cut at an angle to direct the reflection slightly off axis thereby destroying its phase coherence. Another problem can arise when a slight amount of the surface wave energy is scattered within the substrate and converted into bulk acoustic waves which then reflect off the bottom surface of the substrate and interfere with the surface wave on the top(13). This effect is easily reduced by adding grooves or absorbing material to the bottom of the substrate which act to destroy the phase coherence of the bulk acoustic wave energy.

SAW delay line sensors are most easily configured to monitor either changes in the SAW amplitude or SAW velocity. Amplitude measurements are made by using an apparatus described schematically in figure 3. The Rayleigh wave is excited using an RF power source and the power at the

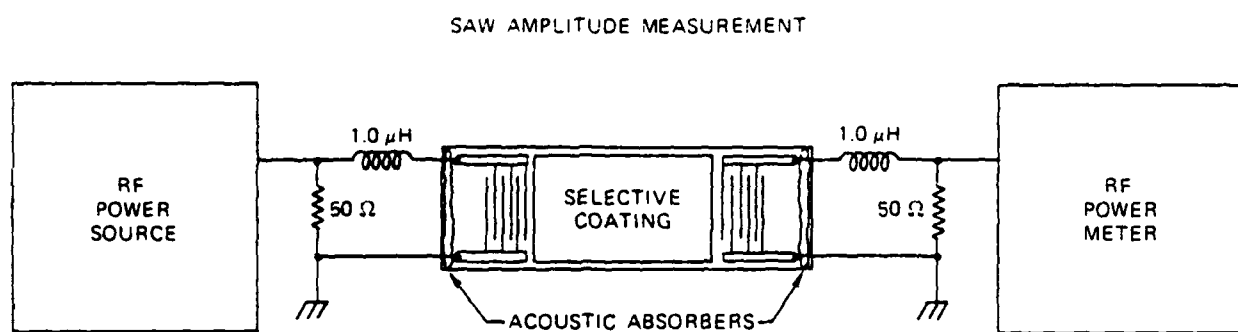


Figure 3. Apparatus used to measure relative SAW amplitudes.

receiving end of the SAW delay line is measured with an RF power meter. More elaborate balanced systems involving a reference device do of course make greater measurement precision possible. Measurements of SAW velocity changes are performed indirectly with extremely good precision by using the SAW delay line as a resonating element. The apparatus required to do this is shown in figure 4. An RF power amplifier is used to feed back energy from the output IDT to the input IDT causing the system to oscillate at the IDT resonant frequency. Oscillations occur only when the amplifier gain is greater than the losses of the delay line. The resonant frequency of the device is altered by changes in the velocity of the Rayleigh wave and can be measured very accurately using a digital frequency counter.

#### THEORY OF SAW INTERACTIONS

##### a) SAW AMPLITUDE PERTURBATIONS

Once a Rayleigh surface wave has been generated by application of an RF voltage at the transmitting transducer it can undergo several types of interactions which can significantly alter the energy content of the wave. In general these lossy interactions will involve either direct absorption of the wave energy or redirection of the energy away from the receiving transducer. In either case the energy of the wave (and hence its amplitude) will be reduced at the receiving transducer and a corresponding reduction in the radio frequency voltage will be observed. Losses in the SAW device substrate arising from scattering at imperfections, viscosity of the crystal and phonon-electron interactions are usually quite small (typically less than 1 db/cm at 100 MHz) and are quite constant with time and moderate temperature fluctuations (e.g.  $\pm 20^\circ\text{C}$ ). Attenuation of the surface wave can also result if a conducting or semiconducting film is placed in contact with



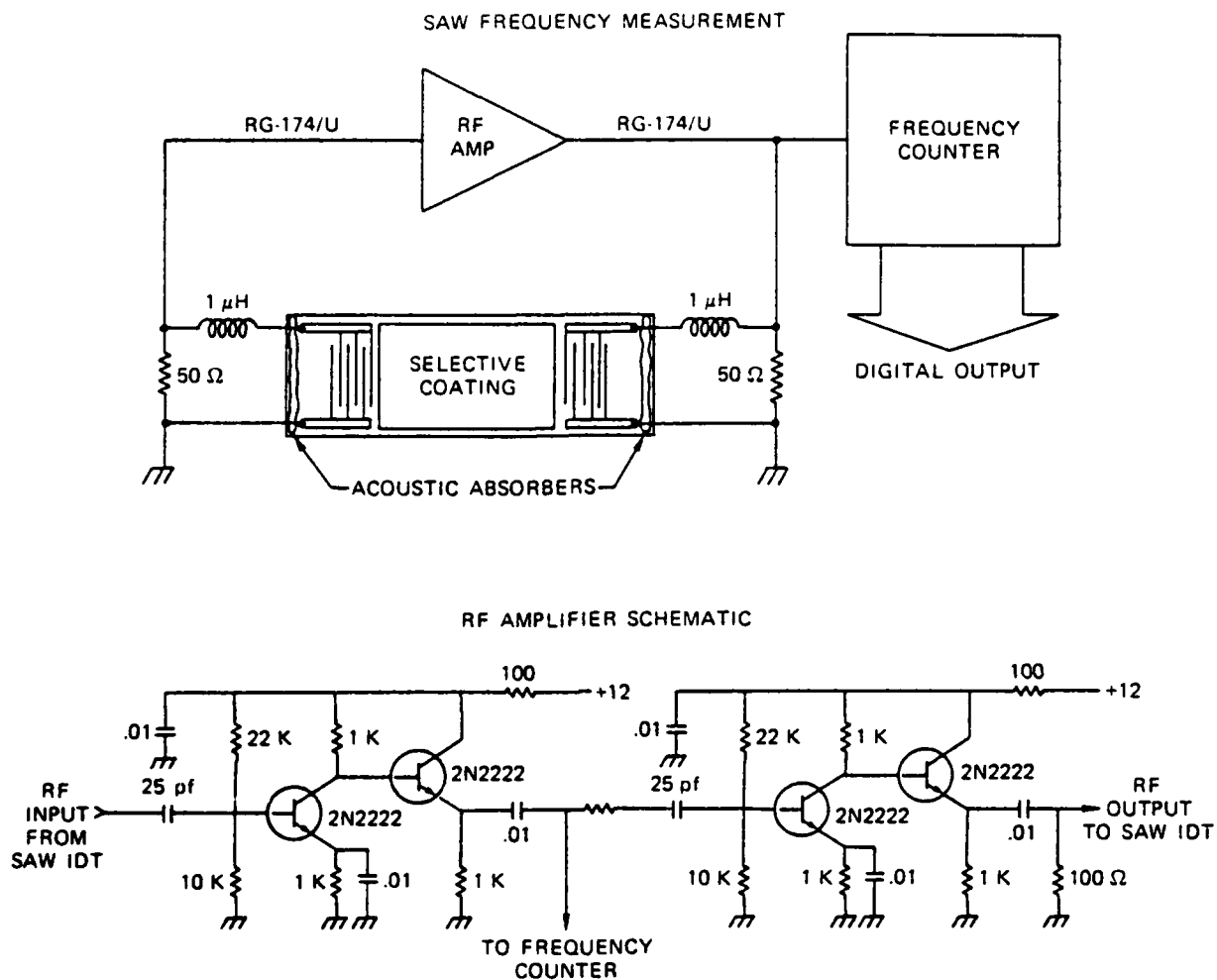


**Figure 4. SAW delay line oscillator system (top) and detailed RF amplifier schematic (bottom).**

the surface since this will short out the electric field associated with the vibrating piezoelectric crystal surface. Ordinarily a metallic film will cause an attenuation of a few decibels per centimeter at 100 MHz. Interactions of the electric field of the surface wave with charge carriers in thin semiconducting films can also result in attenuation of the wave amplitude(14). Surface wave energy is also lost to the ambient gas medium surrounding the SAW device through coupling of the longitudinal component of the acoustic wave on the surface to a corresponding compressional acoustic wave in the gas(15). Losses of less than 1 db/cm at 100 MHz are common.

For chemical microsensor applications the primary interest is in SAW amplitude variations which result when a surface coating (typically a non conducting organic film) adsorbs or absorbs an ambient vapor. Thus all of the previously mentioned sources of attenuation can be regarded as constant. The presence of a thin organic film on the SAW device surface causes attenuation of the wave through interaction with both the longitudinal and vertical shear components of the Rayleigh wave. The mechanism of energy loss from the longitudinal and shear vertical components of Rayleigh waves has been discussed by Dransfeld and Salzmann(16) and their results for longitudinal wave attenuation are used here. A medium in intimate contact with the SAW device surface will experience periodic compression and expansion by the longitudinal wave component at the operating frequency of the device. Since the velocity of sound in the adjacent medium will be different (in fact, lower for gases or organic films) than in the SAW substrate this will result in radiation of compressional wave energy away from the SAW device surface and into the adjacent medium. This energy loss mechanism has an absorption coefficient ( $\alpha_L$ ) given by

$$\alpha_L = \frac{4.3 \rho_F V_F}{\rho V_R \lambda} \text{ db/cm} \quad (1)$$

where  $\rho_F$  is the density of the adjacent medium and  $V_F$  is its velocity of sound;  $\rho$  and  $V_R$  are the density and Rayleigh wave velocity of the SAW substrate and  $\lambda$  is the SAW wavelength. From this equation it should be noted that the attenuation increases with the length of the SAW device and also the inverse of the wavelength (i.e. operating frequency). Implicit in this analysis is the notion that the adjacent medium is thick enough to support compressional waves (i.e. its thickness is greater than  $\lambda$ ). This condition is easily met by ambient gases but for films which are very thin (e.g. thickness less than  $\lambda/100$ ) compressional waves cannot exist and can therefore be neglected from consideration.

Clearly, thick coating films which can support compressional waves (e.g. 100 micron thick film at 31 MHz SAW frequency) will result in a very large attenuation of the Rayleigh wave energy. For vapor sensing applications very thin films are most desirable because rapid equilibration between the vapor and the film would then be possible. Since compressional waves cannot exist in films which are significantly less than one acoustic wavelength thick, the only remaining interaction can be with the vertical shear component of the Rayleigh wave.

Dransfeld and Salzmann(16) have considered the attenuation produced by a purely viscous fluid medium in contact with a propagating Rayleigh wave but their model is of course quite inadequate in predicting the behavior of a thin viscoelastic polymeric film. Tiersten and Sinha(14) and Snider, Fredricksen and Scheider(20) have theoretically investigated the effect of thin metal films on Rayleigh wave attenuation. While neither of these approaches provide results which are rigorously correct for a thin

viscoelastic polymer film, the work of Snider et. al. offers this qualitatively useful result for very thin films of low viscosity:

$$\alpha = A\omega^2\eta h \quad (2)$$

Here  $\alpha$  is the observed attenuation per unit of delay line length,  $A$  is a constant which depends on the film material characteristics,  $\omega$  is the angular frequency of the Rayleigh wave,  $\eta$  is the film viscosity and  $h$  is its thickness. Thus if this relationship is assumed to hold for very thin polymer films, one could expect to observe SAW attenuation which is linearly dependent upon film thickness and viscosity. Enhanced attenuation would also be expected at higher SAW frequencies or for longer delay lines.

#### b) SAW VELOCITY (FREQUENCY) PERTURBATIONS

It was mentioned previously that the most precise measurements of changes in SAW velocity could be made by using the SAW delay line as the resonating element of an oscillator circuit. Determination of the resonant frequency with a precision better than 1 part in  $10^7$  is readily accomplished using a simple digital frequency counter. Stable oscillation in a SAW delay line is obtained when the oscillation frequency ( $\omega$ ) satisfies the following equation(17):

$$\omega = (2n\pi - \phi_e) \frac{V_R}{L} \quad (3)$$

where  $n$  = an integer

$\phi_e$  = electrical phase shift from IDTs and amplifier

$V_R$  = SAW velocity

$L$  = delay line path length between IDT centers

From this relationship it is apparent that many resonant frequencies are possible depending on the value of  $n$ . In practice  $n$  is restricted to only a few values in a simple delay line because of bandwidth constraints imposed by the IDTs. It is possible to design SAW delay line oscillators

which have only one resonant mode(18) but this is not essential for useful SAW sensors. Ordinarily  $\phi_e$  and L are constant (although a slight temperature dependence is sometimes observed). This means that changes in the resonant frequency of a SAW oscillator will occur if the SAW velocity is perturbed through an interaction with a film adjacent to the SAW device surface.

Auld(19) has derived an expression from a perturbation analysis of a SAW device coated with a non conducting, isotropic overlay film which accurately describes the fractional change in wave velocity when the film is very thin (e.g. film thickness is less than 1% of the wavelength).

Auld's resulting equation is:

$$\frac{\Delta V_R}{V_R} = \frac{-V_R h}{4P_R} \left[ \rho' |V_{Ry}|^2 + \left( \rho' - \left( \frac{4\mu'}{V_R^2} \right) \left( \frac{\lambda' + \mu'}{\lambda' + 2\mu'} \right) \right) |V_{Rz}|^2 \right]_{y=0} \quad (4)$$

where h = film thickness (meters)

$V_R$  = Rayleigh wave velocity (m/sec)

$\rho'$  = film mass density (kg/m<sup>3</sup>)

$\lambda'$  and  $\mu'$  = film Lamé' constants (N/m<sup>2</sup>) ( $\lambda'$  = Lamé' const.  $\mu'$  = modulus)

$\frac{(V_{Ry})_{y=0}}{\sqrt{P_R}}$  and  $\frac{(V_{Rz})_{y=0}}{\sqrt{P_R}}$  are the normalized particle velocity components at the surface

This equation can be simplified by setting

$$C_1 = \frac{-V_R |V_{Ry}|^2_{y=0}}{4 P_R} \quad (5)$$

$$C_2 = \frac{-V_R |V_{Rz}|^2_{y=0}}{4 P_R} \quad (6)$$

Thus

$$\frac{\Delta V_R}{V_R} = (C_1 + C_2) h\rho' - C_2 h \left( \left( \frac{4\mu'}{V_R^2} \right) \left( \frac{\lambda' + \mu'}{\lambda' + 2\mu'} \right) \right) \quad (7)$$

However the normalized particle velocity surface components  $|V_{Ry}|^2/V_R^2$  and  $|V_{Rz}|^2/V_R^2$  are frequency dependent and are tabulated by Auld for many SAW substrates in the form of a constant which must be multiplied by the wave frequency (f) in Hertz.

Clearly then  $C_1 = k_1 f$  and  $C_2 = k_2 f$

and

$$\frac{\Delta V_R}{V_R} = (k_1 + k_2) f h \rho' - k_2 f h \left( \frac{4\mu'}{V_R^2} \left( \frac{\lambda' + \mu'}{\lambda' + 2\mu'} \right) \right) \quad (8)$$

Values of  $k_1$  and  $k_2$  for several popular SAW substrate materials are provided in table I. It can also be shown that in the case of a SAW resonator of quiescent frequency f:

$$\frac{\Delta V_R}{V_R} = \frac{\Delta f}{f} \quad (9)$$

Here  $\Delta f$  is the change in resonant frequency due to a perturbation in the wave velocity by a thin overlay film. If the perturbation is small then  $f - \Delta f \approx f$  and the following relationship can be written:

$$\Delta f = (k_1 + k_2) f^2 h \rho' - k_2 f^2 h \left( \frac{4\mu'}{V_R^2} \left( \frac{\lambda' + \mu'}{\lambda' + 2\mu'} \right) \right) \quad (10)$$

It should be noted that the first half of this equation is independent of the shear modulus ( $\mu$ ) and that the quantity  $(\lambda' + \mu')/(\lambda' + 2\mu')$  is in the range of 0.5 to 1.0 with a value of 0.85 being quite typical for many polymeric materials. The shear modulus dependent portion of equation becomes negligible when the quantity  $4\mu'/V_R^2$  is less than 100 (i.e. for "soft" polymers). Thus it is possible to write a simplified relationship between

the resonant frequency of a SAW oscillator and the coating film properties:

$$\Delta f = (k_1 + k_2) f^2 h \rho' \quad (11)$$

The quantity  $h\rho'$  is simply the mass per unit area of the coating film. Small variations in either  $h$  or  $\rho$  will cause a corresponding variation in the oscillator frequency. Also noteworthy is the fact that the magnitude of the frequency change ( $\Delta f$ ) produced by changes in mass per unit area (i.e. sensitivity) is highly frequency dependent. In the case of a 1 micrometer ( $h=10^{-6}\text{m}$ ) thick polymer film ( $\rho = 1000 \text{ kg/m}^3$ ) coating a YX quartz SAW oscillator ( $k_1 = -9.33 \times 10^{-8}$ ,  $k_2 = -4.16 \times 10^{-8} \text{ m}^2\text{-sec/kg}$ ) resonating at 31 MHz, the simplified theory predicts a frequency shift ( $\Delta f$ ) of -129.6 KHz.

TABLE I  
Material Constants for Selected SAW Substrates  
(Derived from Auld (Ref. 19))

| Substrate                               | Rayleigh Wave<br>Velocity |         | $K_1$<br>(m <sup>2</sup> -sec/Kg) | $K_2$<br>(m <sup>2</sup> -sec/kg) |
|---|---------------------------|---------|-----------------------------------|-----------------------------------|
|   | $V_R$                     | (m/sec) |                                   |                                   |
| Y cut X Propagating<br>Quartz           | 3159.3                    |         | -9.33x10 <sup>-8</sup>            | -4.16x10 <sup>-8</sup>            |
| Y cut Propagating<br>LiNbO <sub>3</sub> | 3487.7                    |         | -3.775x10 <sup>-8</sup>           | -1.73x10 <sup>-8</sup>            |
| Y cut 60° x Propagating<br>CdS          | 1702.2                    |         | -8.33x10 <sup>-8</sup>            | -2.67x10 <sup>-8</sup>            |
| 45° Rotated X<br>ZnO                    | 2639.4                    |         | -5.47x10 <sup>-8</sup>            | -2.06x10 <sup>-8</sup>            |
| Z cut X Propagating<br>Si               | 4921.2                    |         | -9.53x10 <sup>-8</sup>            | -6.33x10 <sup>-8</sup>            |



## EXPERIMENTAL SECTION

All of the observations reported here were made with a SAW device designed for operation at 31 MHz. The device was fabricated on an ST quartz substrate (1/2 inch wide and 2 inches long) one side of which was polished (Valpey-Fisher, Inc., Hopkinton, Mass.). The interdigital electrodes consisted of 50 finger pairs of 2000 Å gold on 200 Å chromium. Each finger was 25 micrometers wide and spaced 25 micrometers from the adjacent finger. The finger overlap length was 7250 micrometers. The IDT's were fabricated using standard microfabrication procedures employing an optical lithographic mask exposure of Shipley AZ-1350J photoresist followed by a chlorobenzene soak, development, metal evaporation, and liftoff of the stencil and unused metal. The center to center spacing between the IDT's was 2.0cm. A narrow bead of silicone adhesive was applied to each end of the device to eliminate triple transit echos. Electrical connections to the IDT's were made using metal pressure clips.

Poly (methyl methacrylate) (PMMA), cis poly (isoprene) (PIP), and poly (ethylene maleate) (PEM) were applied to the device by spin coating from solution at 1900 rpm for 1 minute followed by a 5 minute bake at 110°C to drive off residual solvent. Film thickness depended upon polymer solution concentration, solvent and spin speed. Determination of film thickness was done gravimetrically with microscope slides substituted for the SAW device. Spin coating of the microscope slides was performed under conditions identical to those for the SAW device. Measurement of the film mass together with knowledge of the polymer density and microscope slide area allowed a very simple but reliable determination of its thickness.

SAW amplitude measurements were made using a Hewlett-Packard VHF Signal Generator (Model 608 D), a FLUKE Digital Frequency Counter (Model 1910 A)

and a Tektronix oscilloscope (Model 7904). RG-58/U transmission line was used with 50 ohm terminations to minimize reflections. A 1.0 microhenry series inductor was connected to both the input and output IDT's of the SAW device as shown in figure 3. Measurements were made by tuning the signal generator frequency for a maximum signal at the SAW device output as measured with the oscilloscope. The peak to peak RF voltage observed and the signal generator frequency were recorded for a clean SAW device and also for SAW devices coated with progressively thicker films of PEM, PIP, and PMMA.

SAW frequency measurements were made using a simple two transistor class A RF amplifier and an identical buffer amplifier to drive the FLUKE frequency counter. A circuit diagram for this apparatus is shown in figure 4. The resonant frequency of a clean SAW delay line was recorded along with the resonant frequencies for the same device coated with progressively thicker films of PEM, PMMA, and PIP. All measurements were obtained at room temperature and ambient atmospheric pressure.

## RESULTS AND DISCUSSION

### a) SAW AMPLITUDE MEASUREMENTS

The results of measurements of Rayleigh wave amplitude as a function of film thickness are shown in figure 5. The PIP and PEM films both exhibit attenuation which is linearly dependent upon film thickness as predicted by theory (equation 2). The difference in slope between the two polymers is due to the differing film viscosities. PEM which has a glass transition temperature of  $-10^{\circ}\text{C}$  is more elastic than PIP which has a glass transition temperature of  $-70^{\circ}\text{C}$ . A PMMA film whose  $T_g$  is about  $+100^{\circ}\text{C}$  and is less viscous than either PEM or PIP causes the output amplitude of a SAW delay line to increase when compared to a clean delay line. This apparent signal

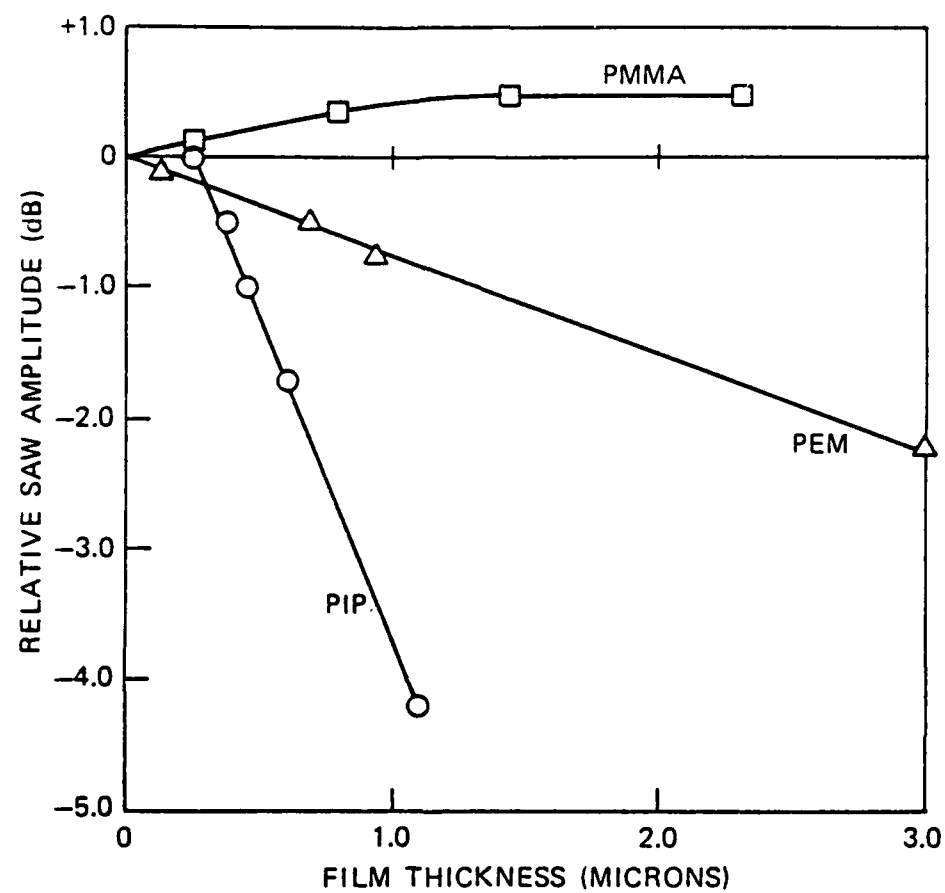


Figure 5. SAW amplitude signal for a device coated with various thicknesses of Poly (methacrylate) ( $\square$ ), Poly (ethylenemaleate) ( $\Delta$ ), and cis-Poly (isoprene) (O). Amplitudes are relative to a clean, uncoated SAW delay line.

enhancement is unexplainable using equation 2 and is probably a result of acoustic energy being guided more efficiently by the film from one IDT to the other. Ordinarily the acoustic beam which is generated by the IDT at one end of the delay line is not completely captured by the IDT at the other. Some of the beam energy is steered off axis due to crystalline anisotropy of the substrate and misses the receiver(11). The film could act as a waveguiding structure to increase the amount of energy captured(19). Because the viscosity of PMMA is low, the relatively small attenuation it provides is more than offset by its waveguiding characteristics, thus resulting in a net signal enhancement. Some evidence for this behavior is also seen in the PIP data which does not go through the origin. Here a film thickness of about 0.25 microns is required to offset the gain in SAW amplitude achieved by waveguiding in the film.

It is appropriate to make several observations on the general problem of measuring surface wave amplitudes. If measurements of SAW amplitudes are being made by driving the device at a fixed frequency with a constant amplitude RF signal and measuring the device output signal amplitude, one must be careful to avoid misinterpretation of the results due to the frequency dependence of the interdigital transducers. The interdigital transducers typically employed for SAW delay lines consist of electrodes of equal length and electrode spacing equal to the electrode width. The frequency response (i.e. the magnitude of the RF voltage present at the output of the delay line as a function of frequency) of such a transducer is described by a  $(\sin x)/x$  function (figure 6). This is simply the Fourier transform of the rectangular spatial distribution of the electrodes. Normally an RF signal is chosen to drive the SAW device which has a frequency near the SAW resonant point where maximum signal transmission

# TYPICAL SAW IDT FREQUENCY RESPONSE

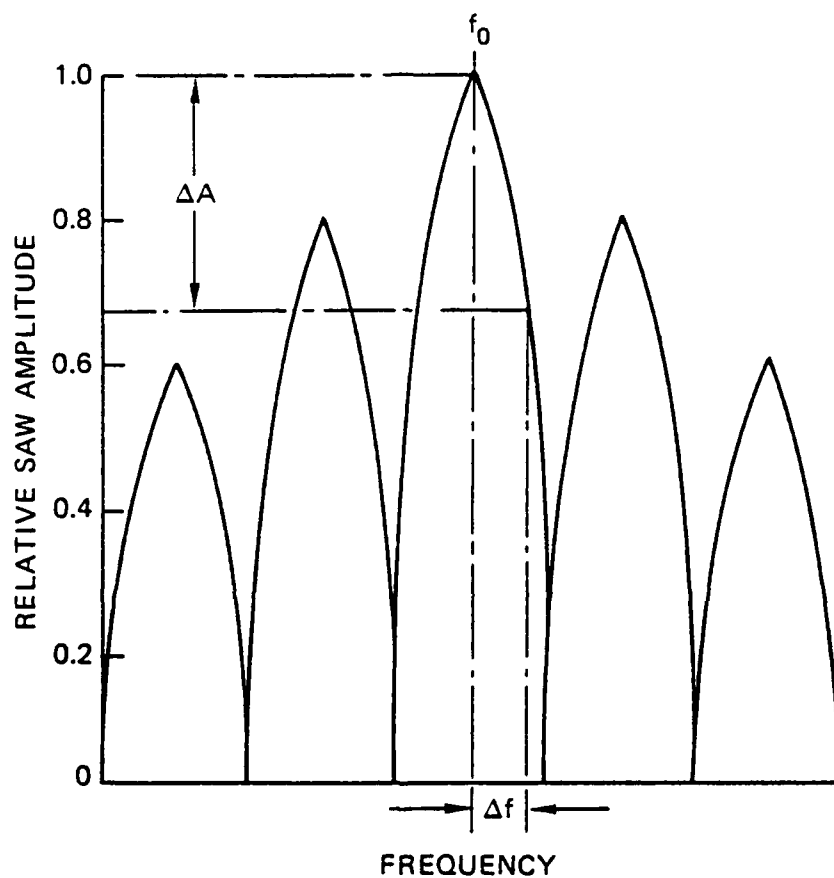


Figure 6. Characteristic frequency response of a simple SAW IDT electrode. Small differences ( $\Delta f$ ) between the resonant frequency of the IDT ( $f_0$ ) and the frequency of the RF voltage source can result in very large shifts in the amplitude ( $\Delta A$ ) which can confuse the interpretation of SAW amplitude measurements.

through the delay line occurs. As will be shown in the next section, the resonant frequency of a SAW delay line is quite sensitive to changes in the medium coating the delay line surface. Thus even in the absence of changes in the acoustic absorption characteristics of the coating, a change in amplitude can be observed if the resonant frequency of the delay line changes while it is being driven at a fixed frequency. Indeed this is a convenient way to produce a voltage change instead of a frequency change when the resonant characteristics of the delay line are altered. If this effect is to be minimized then a transducer of large bandwidth (i.e. few finger pairs) must be employed. Conversely if a large change in voltage amplitude is desired for a small change in resonant frequency then a very narrow bandwidth transducer (i.e. many finger pairs) is most desirable. Precise measurement of the absolute attenuation produced by a coating film interaction will require measurement of the RF voltage magnitude at the delay line output when the frequency of the input RF voltage has been adjusted to correspond with a predetermined resonance maximum of the delay line. Thus the frequency of the driving RF voltage will not always be fixed but rather slightly variable depending on the amount of the detuning produced by coating. Alternatively, a resonant oscillator system could be employed and the amplitude of the voltage at the delay line output could be monitored.

An estimate of the ability to detect vapors using SAW amplitude changes can be obtained if one assumes that the sorption of a vapor by the coating film can be regarded as an incremental change in its thickness. Using a cis poly (isoprene) film (1cm wide x 2cm long) as an example, the slope of the attenuation vs thickness curve is approximately -4 db/micron at 31 MHz. It is possible (although not trivial from an instrumentation standpoint) to

measure attenuation changes of  $\pm 0.001$  db in an RF signal at 31 MHz. Thus, a change in thickness of  $2.5 \times 10^{-4}$  micron on this  $2\text{cm}^2$  surface film would be detectable. This corresponds to about 50 nanograms of material.

Considerably lower detectabilities are possible at higher operating frequencies, however, the primary limitation will be in the instrumentation required to perform the precise SAW amplitude measurements. The greater instrumental complexity and (as it will be shown), the lower sensitivity of the SAW amplitude measurements compared to SAW frequency measurements makes the amplitude approach less interesting for sensor applications at this time.

#### b) SAW FREQUENCY MEASUREMENTS

The frequency shifts obtained from a 31 MHz ST-Quartz SAW oscillator with various coating thicknesses of poly (methyl methacrylate), poly (isoprene), and poly (ethylene maleate) are shown in figures 7 to 9, respectively. These curves and the response predicted by equation 11 (for YX quartz) are displayed on the same axis in figure 10. The responses obtained for PEM and PMMA are quite similar and lie within the envelope of theoretically predicted response for films whose densities are in the range of 0.7 to 1.3 gm/cc. The behavior of the PIP is slightly different from that of the other two films studied and this could be related to its "softer" viscoelastic properties (i.e. smaller elastic modulus) although the exact cause is not known. Considering the number of assumptions and simplifications required to arrive at equation 11, the theoretical results are in very good agreement with experimental results. The theoretical responses were obtained using material constants ( $k_1 + k_2$ ) for YX quartz since constants for ST quartz were not available. It is believed that the constants for YX and ST quartz should be quite similar. The scatter

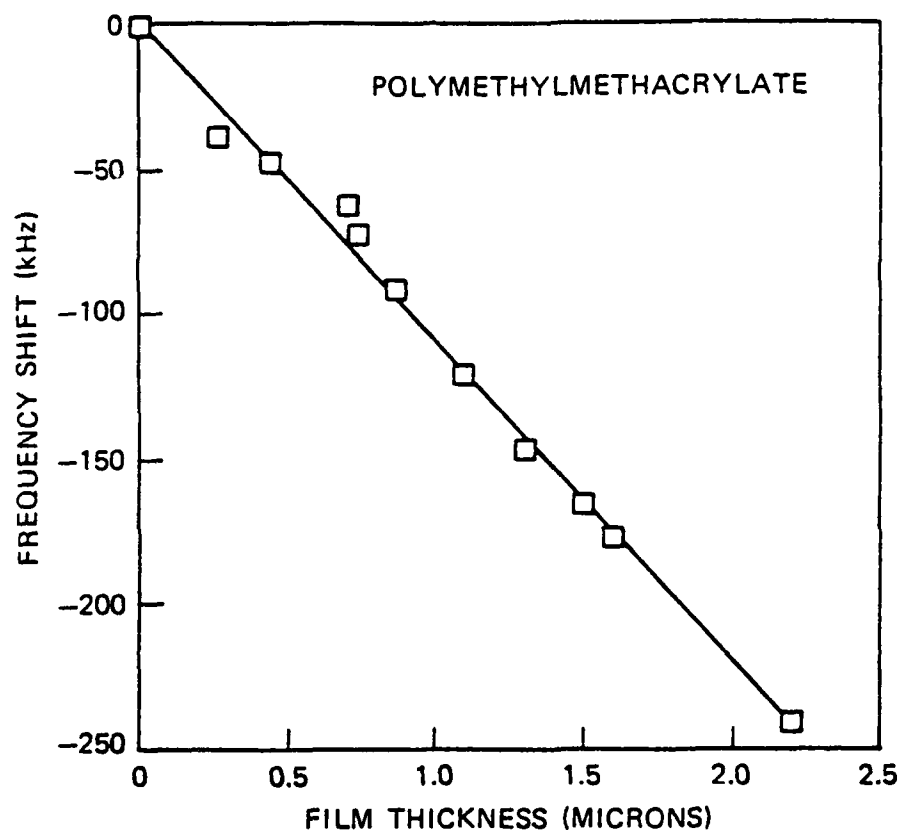


Figure 7. SAW oscillator frequency shift produced by various thicknesses of Poly (methyl methacrylate).



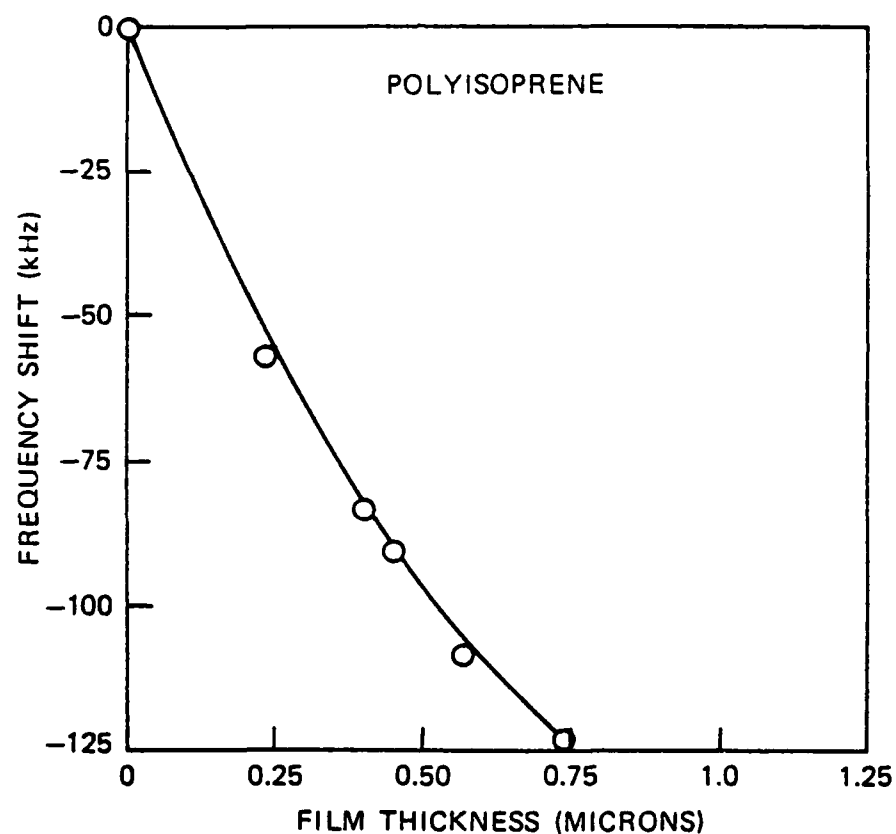


Figure 8. SAW oscillator frequency shift produced by various thicknesses of *cis*-Poly (isoprene).

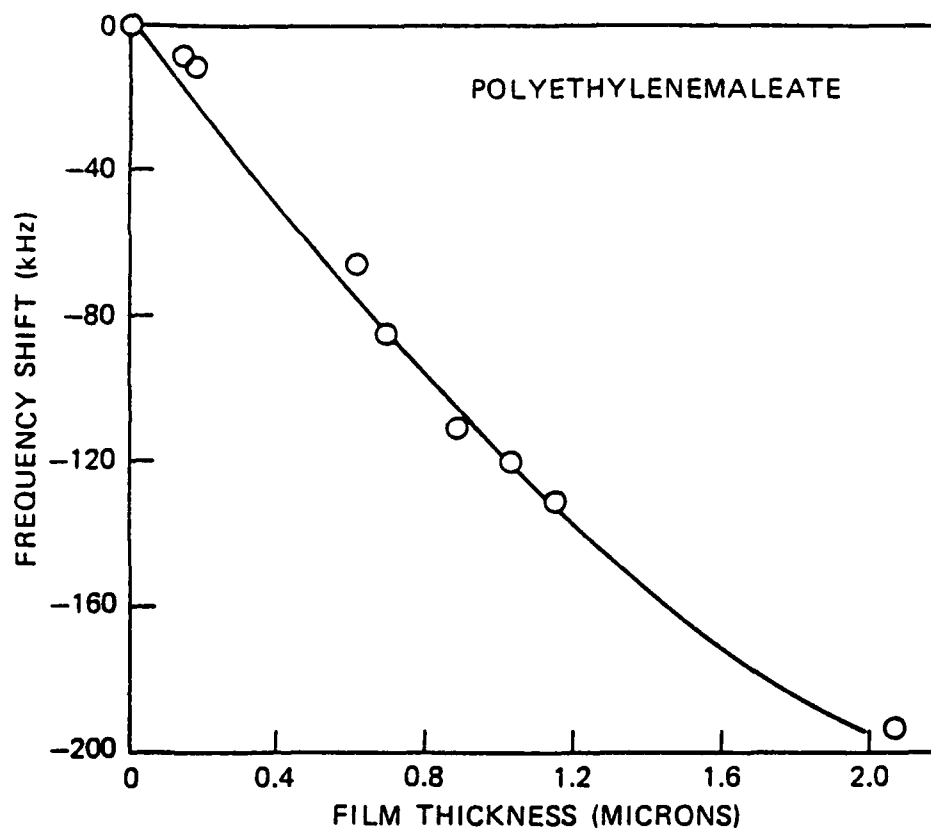


Figure 9. SAW oscillator frequency shift produced by various thicknesses of Poly (ethylene maleate).

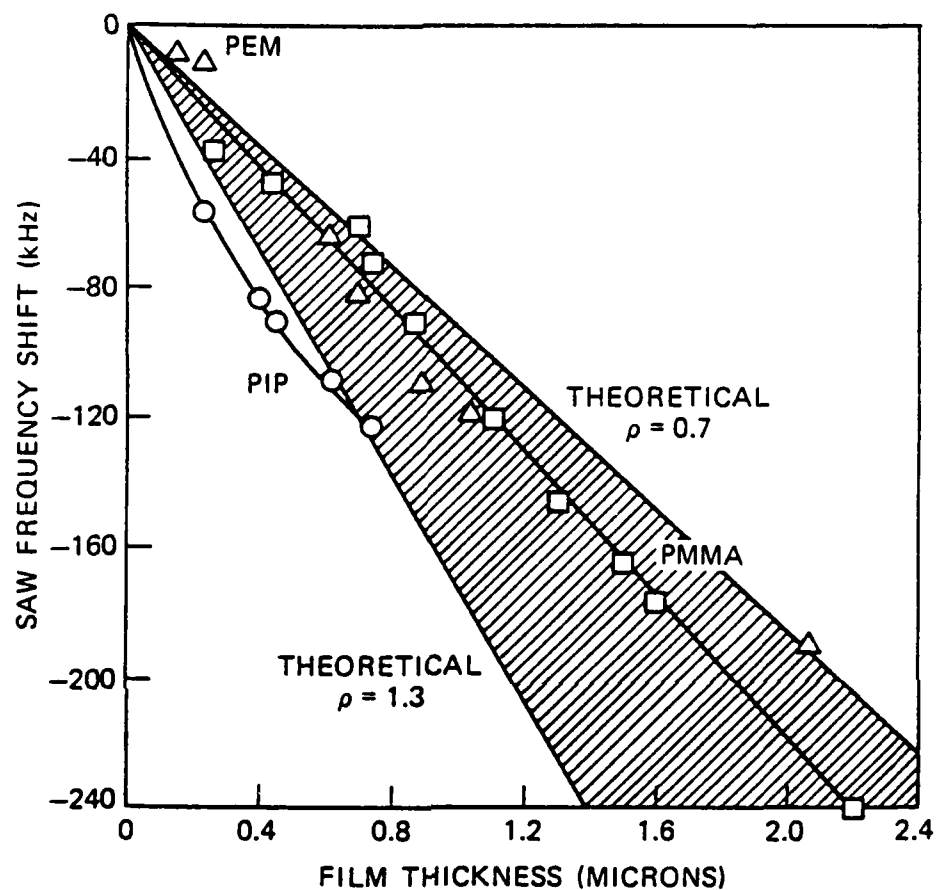


Figure 10. SAW oscillator frequency shifts produced by Films of Poly (ethylene maleate) ( $\Delta$ ), cis-Poly (isoprene) (O), and Poly (methylmethacrylate) ( $\square$ ) compared with response predicted by equation 11. Shaded region shows the theoretical frequency shift assuming a film density ( $\rho$ ) in the range of 0.7 to 1.2 gms/cc.

observed in the frequency shift vs film thickness data is primarily a result of errors in the gravimetric determination of film thickness. Frequency shifts produced by the films could be measured with a precision of 1 hertz. Under typical conditions (i.e. ambient temperature and pressure) the baseline noise observed from the 31 MHz SAW oscillator was less than  $\pm 1$  hertz RMS. The sensitivity of the SAW oscillator can be appreciated by considering that a 1 micron thick film of PMMA produced a frequency shift of greater than 100 KHz. This means that film thickness variations of about 0.1 Å are measurable.

The signal generated by a sensor for a given stimulus (i.e. sensitivity) is not its only important characteristic. From the point of view of detectability the signal to noise ratio is most important. In a SAW delay line oscillator signal, noise appears as random or drifting frequency fluctuations. Drift results from slow thermal changes in the SAW device substrate and electronic amplifier. The resonant frequency ( $\omega$ ) of a SAW delay line oscillator is given by equation 3 where the ratio ( $V_R/L$ ) is equal to the reciprocal of the delay time (i.e.  $1/\tau$ ). One can readily see that if the temperature of the substrate changes then the delay time will change due to the linear thermal expansion coefficient of the substrate. This results in a temperature dependent frequency shift. ST quartz is a material which has a temperature coefficient of delay  $\frac{1}{\tau} \frac{\delta \tau}{\delta T}$  which is nearly zero at room temperature and is thus very desirable for sensor applications. Use of other substrates with nonzero temperature coefficients of delay (e.g.  $\text{LiNbO}_3$ ) will result in greater temperature drift which may require compensation with a reference device or oven. Also apparent is the fact that small changes in the phase shift of the electronic amplifier ( $\phi_0$ ) due to thermal variations in the components will show up as frequency drift.

The relative change in frequency for a change in amplifier phase shift was shown by Ash to be (18):

$$\frac{\delta f}{f} = \frac{-\delta \phi}{2\pi n} e \quad (12)$$

Here the factor  $2\pi n$  is analogous to the  $Q$  of the resonator and as the resonator  $Q$  increases (by increasing the delay line length and hence  $n$ ) the effect of amplifier phase shift variations can be greatly reduced.

The random frequency noise encountered in SAW delay line oscillators results from Johnson type thermal noise present at the input of the RF amplifier. Lewis has considered the problem of the short term stability of a SAW delay line oscillator system(17) and has developed an expression describing the output power spectrum of such an oscillator.

$$S_{RF}(\omega) \approx \frac{(2/\pi) kT(NF)G^2}{\left[ \frac{2kT\omega_0}{P_o Q} \right]^2 + \left[ \frac{Q(\omega - \omega_0)}{\omega_0} \right]^2} \quad (13)$$

where

$S_{RF}(\omega)$  = Power spectrum magnitude

$k$  = Boltzmann's const.

$T$  = Absolute temperature

$NF$  = Amplifier noise figure

$G$  = Amplifier gain

$\omega_0$  = SAW resonant freq.

$Q$  = System quality factor

$P_o$  = output power

For the maximum stability (i.e. minimum frequency noise) of a SAW oscillator it is desirable that the output power spectrum be small at all frequencies ( $\omega$ ) different from the resonant frequency ( $\omega_0$ ). Thus by inspection of the above equation one readily sees that the most stable system will result when amplifier noise figure ( $NF$ ) is low, the amplifier gain (which is required to compensate for the delay line losses) is low, the

output power ( $P_o$ ) and delay line Q are high. Under these conditions the sharpest resonance will be obtained. The amplifier output power and noise figure can be considered as factors independent of the SAW delay line. The amplifier gain required to produce oscillation and the system Q are heavily dependent upon the losses experienced by SAW delay line. A thick coating film on a SAW oscillator vapor sensor could have the result of absorbing a larger amount of energy from the device which necessitates a correspondingly larger amplifier gain. Furthermore, the Q (which is classically defined as the ratio of energy stored to the energy dissipated per oscillation cycle) will also be greatly reduced. While a thicker coating film could have the ability to interact with more vapor and generate a greater signal, it could also have the effect of increasing the baseline noise. Thus it appears that for a given sensor an optimal coating thickness will exist which provides a maximum signal to noise ratio.

From the preceeding considerations it should be clear that careful attention must be given to the design of the SAW delay line and its RF amplifier in order for optimal performance to be achieved. The delay line should have low insertion loss. This can be accomplished by having a large number (e.g. 50) pairs of interdigital electrodes and series inductors accurately tuned with them to achieve maximum power transfer with the RF amplifier. The RF amplifier itself should be operated with moderate gain (e.g. 20db) and should have a low noise figure (e.g. 3db at 100 MHz). Proper heat sinking of the RF amplifier will help to minimize thermally induced electronic phase shift variations.

#### (c) SAW VAPOR SENSOR CONSIDERATIONS

The results obtained from the amplitude and frequency studies of polymer coated SAW delay lines indicate that the SAW oscillator approach

offers the best signal to noise ratio. A 0.5 micron thick film of cis poly isoprene was observed to produce an attenuation of approximately 1.2 db and a frequency shift of approximately 100 KHz. Considering that the baseline noise achievable in an RF amplitude measuring system is about  $\pm 0.001$  db and the observed baseline line noise in the frequency measurement system was about  $\pm 1$  Hz, it is apparent that the frequency measurement system offers the highest signal to noise ratio (i.e. 100,000 vs 1,200). This result together with the simpler apparatus requirements and the moderately accurate theoretical model of the SAW delay oscillator makes it the most attractive vehicle for vapor sensing applications.

It has been shown that the SAW delay line oscillator is sensitive to both the mass per unit area of material present on the surface wave device and to the mechanical properties of the material (equation 10). No direct sensitivity to a vapor is indicated. For this reason a coating film is required to convert this mass sensitive device into a vapor concentration sensitive device. The coating, through either physisorption or chemisorption must interact selectively with the vapor of interest to cause a change in mass or mechanical property of the coating. While the SAW oscillator is easily capable of detecting monolayer adsorption onto its surface, greater sensitivity can be obtained by using a thicker coating film through which the vapor can diffuse and interact with a greater number of sorption sites than on a smooth surface. Vapor diffusion rate and device response time are closely related. Clearly a film which is very dense will not permit easy diffusion and the device will respond very slowly.

For polymeric coatings rapid diffusion is most easily obtained if the polymer is highly amorphous and well above its glass transition temperature. For such a film the shear modulus is probably small enough to

make its mechanical contribution to the SAW oscillator frequency a negligible quantity. Thus, for vapor permeable films equation 11 will be the most accurate predictor of SAW frequency shift. Incremental changes in film density or thickness (i.e. mass per unit area) will result in a corresponding resonant frequency change. Coatings such as thin liquid films which can interact with a vapor will also work on the SAW device. However, the volatility of most liquids is high enough to cause a steady baseline drift due to evaporation. Coatings developed for bulk wave piezoelectric crystal vapor sensors will also work with the SAW device (22,23).

The reversibility of the coating will depend entirely on the nature of the vapor/coating interaction. Interactions involving chemisorption will usually be quite selective but irreversible under normal conditions and will be most useful in dosimetry applications where an integral signal related to the concentration and time of exposure to a particular vapor is desired. The large dynamic range capability of the SAW oscillator and the low cost of the device permit irreversible interactions to be considered as a practical system. For reversible responses, interactions involving physisorption will be required. Unfortunately the relatively low energies of adsorption associated with physisorption processes could permit several different vapors with similar properties to interact with the coating film. Thus it is possible that the coating specificity and reversibility will be conflicting requirements. One possible solution to the specificity problem could involve the use of multiple sensors with different coatings to allow compensation for known interferences. Once again the attractive characteristics of the SAW device (i.e. very small size and low cost) make this approach practical.



(d) ULTIMATE PERFORMANCE LIMITS

The sensitivity and size of SAW delay oscillator sensors is directly related to their resonant frequency. Equation 11 predicts that the frequency shift obtained for a given mass loading will increase with the square of the operating frequency. Thus, a device operating at 3 GHz will exhibit frequency shifts 10,000 times greater than a 30 MHz device for the same mass loading. However, it is expected that the baseline noise for the 3 GHz device will also be somewhat higher resulting in a signal to noise ratio which is less than 10,000 times greater. It is interesting to note that the frequency shift obtained for a given mass loading is independent of the length of the SAW delay line. The baseline noise, however, depends on the effective delay line Q which is related to the length of the device. Thus, longer delay lines will produce higher signal to noise ratios not by increasing the signal but rather by decreasing the noise. The SAW delay line oscillators used in this study operating at 31 MHz had a delay line length which supported about 300 cycles of the Rayleigh wave between the IDT electrodes. The Q of these devices was high enough to provide frequency noise less than 1 Hz (i.e. stability of better than 1 part in  $10^7$ ). If one can maintain the same numbers of cycles (i.e. wavenumber) between the IDTs at other frequencies then comparable stabilities should result. Thus the baseline noise is expected to increase linearly with frequency (i.e. stay at 1 part in  $10^7$ ) whereas the signal increases with the square of the frequency. The overall result is a signal to noise ratio which increases linearly with frequency.

The area occupied by the device is also frequency dependent. On ST quartz the IDT aperture width (i.e. electrode overlap length) should be about 28 wavelengths (11) to provide a 50 ohm impedance frequently required

by the RF amplifier. If a constant wavenumber is maintained, then the device length will also depend on the wavelength. Thus, the area of a SAW delay line with constant IDT impedance and wavenumber will vary inversely with the square of the operating frequency. The reduction of device area also has implications with regard to the minimum mass change that can be detected by a SAW delay line oscillator. Since the device is sensitive to mass per unit area, a reduction in device area results in a corresponding reduction in the minimum detectable mass change. A summary of estimated SAW device sensor performance at various operating frequencies is presented in Table II. Detection of a few femtograms of material with a 3 GHz device having  $10^{-4}$  cm<sup>2</sup> of active area seems theoretically possible.

The fabrication of SAW devices to operate at frequencies up to 3 GHz poses no significant technical challenge. Optical lithographic techniques will easily produce devices operating around 300 MHz. For higher frequencies, e-beam or x-ray lithography systems would be required but the process would still be very simple since only a single level of pattern masking is needed. Above 300 MHz the main challenge will be to develop suitable RF amplifiers and electrical connecting leads to permit stable device operation.

There are numerous piezoelectric materials which can be used as a SAW device substrate. From inspection of Table I it appears that quartz is a good choice since the constants  $k_1$  and  $k_2$  are relatively large which results in greater sensitivity (equation 11). It is also practical to consider thin piezoelectric films deposited on a silicon wafer (10). Such an approach would allow many devices to be fabricated in one step resulting in lower cost. Other SAW devices besides the delay line oscillator could also be

TABLE II

## Estimated SAW Device Sensor Performance

| Frequency | Device Area <sup>1</sup>         | Baseline Noise <sup>2</sup> | Minimum Detectable<br>Mass Change <sup>3</sup> |
|-----------|----------------------------------|-----------------------------|--|
| 30 MHz    | 1 cm <sup>2</sup>                | 3 Hz                        | 3 x 10 <sup>-9</sup> gm                        |
| 300 MHz   | 10 <sup>-2</sup> cm <sup>2</sup> | 30 Hz                       | 3 x 10 <sup>-12</sup> gm                       |
| 3 GHz     | 10 <sup>-4</sup> cm <sup>2</sup> | 300 Hz                      | 3 x 10 <sup>-15</sup> gm                       |

## Notes:

1. Approximate area required to produce a delay line on ST Quartz with 50 ohm IDT impedance and a cavity wavenumber of 300.
2. Assuming a SAW oscillator stability of 10<sup>-7</sup>.
3. Minimum mass change required to produce a signal plus noise to noise ratio of 2 (S+N/N = 2). Frequency shift based on Eq. 11.

useful as sensors. In particular, the SAW resonator device could offer some advantages over the delay line particularly at higher frequencies (18).

The SAW vapor sensor is similar to the bulk wave piezoelectric quartz crystal vapor detector originally developed by King (21) and extensively investigated by Guilbault et. al. (22,23). Both are mass sensitive and require a selective coating; both use a shift in resonant frequency as the indicating signal. However, there are several significant differences which deserve mention. First, the SAW device is capable of operating at frequencies which are at least two orders of magnitude higher than the bulk wave device and is therefore capable of much greater sensitivity. Second, the planar geometry of the SAW device allows one side to be rigidly mounted making it even more rugged than the bulk wave devices. Third, the device is intrinsically a micro sensor with its ability to occupy a volume as small as a few nanoliters. Finally, the SAW device allows multiple sensors to be fabricated close together on the same substrate. Thus, temperature drift compensation using a reference device can be achieved with great precision.

Equation 11 permits a direct comparison to be made between the sensitivities of bulk wave piezoelectric quartz crystal oscillator vapor sensors and SAW vapor sensors. Sauerbrey(24) was the first to develop an analytical expression which describes the frequency shift obtained from a bulk wave crystal oscillator under a given mass loading. King reported (21) that for quartz, the Sauerbrey equation is:

$$\Delta f = 2.3 \times 10^6 f_0^2 (\Delta W/A) \quad (14)$$

where  $f_0$  is the quiescent resonant frequency of the oscillator (in MHz),  $\Delta W$  is the change in mass of the crystal (in grams) and  $A$  is the area of the crystal (in  $\text{cm}^2$ ). Equation 11 can be reconstructed to fit the same form as the Sauerbrey equation if one realizes that the product of film thickness

(h) and density ( $\rho$ ) is simply the mass per unit area. For a YX quartz SAW delay line oscillator the frequency shift resulting from a given mass loading can be described by the following equation:

$$\Delta f = 1.3 \times 10^6 f_0^2 (\Delta W/A) \quad (15)$$

At first glance the bulk wave oscillator appears to be the most sensitive since it will produce the greater signal ( $\Delta f$ ) for a given frequency and mass loading. However, bulk wave oscillators with fundamental mode resonant frequencies of greater than 15 MHz are quite difficult to fabricate and very fragile in operation due to the extremely small crystal thickness required. SAW devices and their associated electronics are very easy to fabricate and operate at 300 MHz and, with carefully designed electronics, can go to 3 GHz. Thus, the SAW device offers the highest possible sensitivity due to its higher operating frequency.

A direct comparison between a 15 MHz bulk wave oscillator and a 300 MHz SAW oscillator shows that the SAW device should produce a frequency shift which is more than 200 times greater than the bulk wave device under identical mass loading (i.e. mass per unit area).

### CONCLUSION

The effects of various coating film thicknesses on the amplitude and velocity of propagating Rayleigh surface waves has been studied experimentally and compared with theory. For a given film loading, the measurement of SAW velocity with a delay line oscillator system afforded the greatest sensitivity to film variations. If a vapor of interest perturbs the mass of the selective coating film by diffusing into the film and either chemisorbing or physisorbing then the mass loading on the SAW device will increase, resulting in a wave velocity reduction and a corresponding

downward shift in the delay line resonant frequency. A highly simplified analytical expression has been derived from theoretical considerations which predicted SAW delay line oscillator frequency shifts for a given mass loading. In spite of its many simplifying assumptions, reasonably good agreement with experimental data was obtained. Thus, the mechanism of operation of the SAW vapor sensor has been shown to be quite similar to that of the bulk wave piezoelectric quartz crystal vapor sensor. The significantly higher operating frequencies obtainable with the SAW device results in a sensitivity which is theoretically orders of magnitude greater than that of the bulk wave device. The high sensitivity of the SAW device, together with its low cost, small size, ruggedness, and electronic output make it very attractive for application in a broad spectrum of vapor phase analytical problems. The ultimate success of these devices appears to be limited only by the performance of the selective coating films. In practical systems it may be necessary to compensate for interference vapors by using an array of devices with different coatings. The planar geometry and small size of the SAW vapor sensor makes it an ideal vehicle in such a system.

#### ACKNOWLEDGMENT

The author wishes to thank Dr. N. L. Jarvis and Dr. A. Snow of the Naval Research Lab for many helpful discussions during the course of this work.

# LITERATURE CITED

1. Lord Rayleigh, Proc. London Math. Soc. 1885, 17, 4.
2. White, R.M.; Voltmer, F.W. Appl. Phys. Lett. 1965, 7, 314.
3. White, R. M. Proc. IEEE 1970, 58, 1238.
4. ——— Proc. IEEE 1976, 64, 579.
5. Wohltjen, H. "Methods of Detection with Surface Acoustic Wave and Apparati Therefor" 1982, U. S. Patent No. 4,312,228.
6. Wohltjen, H.; Dessy, R. Anal. Chem. 1979, 51, 1458.
7. Fertsch, M.T. Masters Thesis, U.C. Berkeley, Berkeley, CA, 1980.
8. Fertsch, M.T.; White, R.M.; Muller, R.S. Presented at The Device Research Conference, Ithaca, N.Y., 1980.
9. Bryant, A.; Lee, D.L.; Vetelino, J.F. Proc. 1981 Ultrasonics Symp., IEEE Cat. 81CH1689-9, 171.
10. Chuang, C.T.; White, R.M.; Bernstein, J.J. IEEE Elec. Dev. Lett. 1982, EDL-3, 145.
11. Morgan, D.P. Ultrasonics 1973, V. 11, May, 121.
12. D'Amico, A.; Palma, A.; Verona, E. Appl. Phys. Lett. 1982, 41, 300.
13. Wagers, R.S. Proc. IEEE 1976, 64, 699.
14. Tiersten, H.F.; Sinha, B.K. J. Appl. Phys. 1978, 49, 87.
15. Slobodnik, A.J. Jr., J. Appl. Phys. 1972, 43, 2565.
16. Dransfeld, K.; Salzmman, E. "Physical Acoustics Vol VII"; Mason & Thurston eds., Academic Press: New York, 1970; pp 219-272.
17. Lewis, M.F., Ultrasonics 1974, 12, 115.
18. Ash, E.A. "Acoustic Surface Waves"; A.A. Oliner ed. Springer-Verlag: New York, 1978; pp 117-124.
19. Auld, B.A. "Acoustic Fields and Waves in Solids, Vol. II"; Wiley-Interscience: New York, 1973; chap. 12, pg. 271 - 332.
20. Snider, D.R.; Fredricksen, H.P.; Schneider, S.C. J. Appl. Phys. 1981, 52, 3215.

LITERATURE CITED (CONT'D)

21. King, W.H. Jr., Anal. Chem. 1964, 36, 1735.
22. Tomita, Y.; Ho, M.H.; Guilbault, G.G. Anal. Chem. 1979, 51, 1475.
23. Hlavay, J.; Guilbault, G.G. Anal. Chem. 1978, 50, 1044.
24. Sauerbrey, G. Z. Physik. 1959, 155, 206.



REND

FILMED

1/1

ADAMK